Composition-tuned optical properties of $CdSe_xS_{1-x}$ and $CdSe_xS_{1-x}$/ZnS QDs*

WU Feng, ZHANG Siwen, TIAN Zhu, YU Wenhui, SUN Shishuai, and LI Xiaolan**

Department of Physics, School of Science, Tianjin University of Technology, Tianjin 300384, China

(Received 10 December 2021; Revised 12 May 2022)

The different compositions of the ternary alloyed $CdSe_xS_{1-x}$ quantum dots (QDs) and $CdSe_xS_{1-x}$/ZnS core/shell quantum dots (CSQDs) have been synthesized by the chemical routes. The radii of these QDs were determined by transmission electron microscope (TEM). The optical properties of these QDs were investigated by the absorption and fluorescent measurement. It was found that the absorption and fluorescent emissions were tuned by the component ratio, and the Commission Internationale de l´Eclairage (CIE) coordinates of the fluorescent spectra also depended on the composition. Compared with the $CdSe_xS_{1-x}$ QDs, the $CdSe_xS_{1-x}$/ZnS CSQDs exhibit the fluorescence enhancement due to the surface passivation by shell coating. The composition-tuned optical properties may allow them to be used as fluorescent markers in biological imaging and to fabricate multicolor light emitting diode (LED).

Document code: A **Article ID:** 1673-1905(2022)08-0479-5

DOI https://doi.org/10.1007/s11801-022-1188-5

Semiconductor nanocrystals (NCs) known as quantum dots (QDs) are composed of an inorganic core, made up of a few hundred or a few thousand atoms. In recent years, the rapid developments in the fabrication of QDs have pushed forward the investigations of their chemical and physical properties[1-3]. Confinement effects make them possess remarkably different optical properties from the bulk, such as size-tunable absorption, narrow band fluorescence and large optical nonlinearity. These unique optical properties allow them to be potentially applied in biological and optoelectronics fields. So QDs are still one of great concerns in both research and application fields so far[4,5].

The tunable absorption and narrow band fluorescence are essential for the application in the photoelectric device and biological imaging[6-9]. From the fundamental physical point of view, the narrow bandwidth of the fluorescence is easier to be obtained from the II-VI semiconductor than the III-V QDs under the same size distribution on account of the large hole effective mass in the II-VI semiconductor QDs. Thus, the optical properties of II-VI semiconductor QDs still have attracted a widespread attention recently[10]. For the specific surface of QDs, these QDs are readily degraded as a function of time due to a surface oxidation. Moreover, the suspended bonds on the surface of the QDs result in the defect states, which have a great impact on the optical properties of QDs. In order to improve the optical properties, the wide bandgap semiconductor shell encapsulated on core QDs is often adopted as an effective method for the improvement of optical performance. Recent reports show that the core/shell structure can increase the photoluminescence quantum yield to some extent[11]. Previous reports have been focused on the size-tuned optical properties[12-14]. Compared with the method of the sized-tunable optical properties, the composition-tuned method is easier to realize the control of the optical properties for these ternary alloy QDs. Nevertheless, there are few reports on the composition-tuned optical properties of $CdSe_xS_{1-x}$ QDs and $CdSe_xS_{1-x}$/ZnS core/shell quantum dots (CSQDs). In this letter, we synthesized the ternary alloyed $CdSe_xS_{1-x}$ and $CdSe_xS_{1-x}$/ZnS CSQDs with different compositions. The optical properties of these QDs were investigated by the absorption and fluorescent measurement. It was found that the absorption fluorescent emission was tuned by component ratio and the Commission Internationale de l´Eclairage (CIE) coordinates of the fluorescent spectra also depended on the composition. The composition-tuned optical properties may lead to a wide application in the photoelectric and biological fields.

The ternary alloyed $CdSe_xS_{1-x}$ QDs and $CdSe_xS_{1-x}$/ZnS CSQDs with different compositions have been synthesized by the chemical routes. The three samples of $CdSe_xS_{1-x}$ QDs were prepared and their feed mole ratios of Cd, Se and S are 1: 0.28: 29.02, 1: 0.50: 26.69 and 1: 0.81: 24.58. According to their feed mole ratios, these $CdSe_xS_{1-x}$ QDs samples were labeled as S1, S2 and S3 and their CSQDs counterparts labeled as S1', S2' and S3'. The detailed preparation process was described in our

* This work has been supported by the National Natural Science Foundation of China (No.11204214), and the Teaching Reform Project of Tianjin University of Technology (No.ZX20-05).

** E-mail: ourdaywufeng2000@163.com

previous work[15]. At last, these QDs were dissolved in some amount of chloroform and their concentration was 5×10^{-3} mol/L. The sizes of $CdSe_xS_{1-x}$ QDs and $CdSe_xS_{1-x}$/ZnS CSQDs were inspected by the transmission electron microscope (TEM, Philip TZOST) operating at 190 kV. The linear absorption spectra of these QDs were recorded on the ultraviolet-visible (UV-Vis) spectrometer (TU-1901). The fluorescent emission spectra of these QDs were recorded on the fluorescence spectrometer (F4500).

The TEM image of $CdSe_xS_{1-x}$ QDs in the sample S2 is shown in Fig.1(a), and the size distribution is presented in Fig.1(b). The solid line is a Gaussian fitting result to the size distribution, and the average diameter is (4.0±0.2) nm as shown in Fig.1(b), which is consistent with the determined size of S1 in our previous report[15]. The TEM images and the size distributions of the other samples are similar to those of S2, which are not given here.

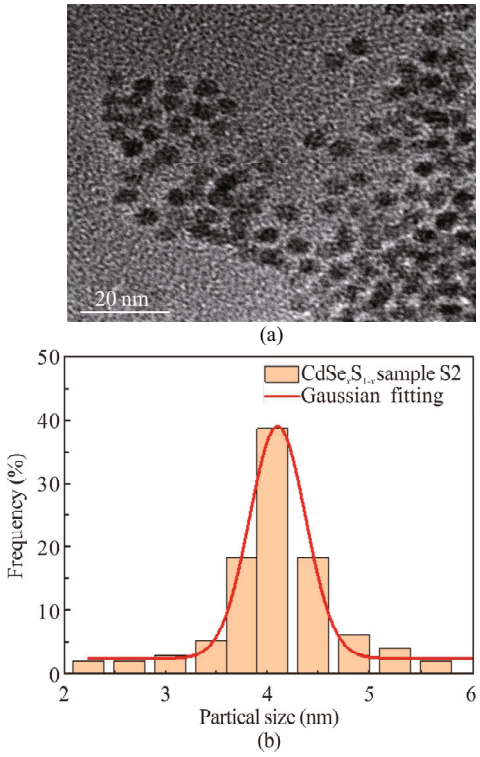

Fig.1 (a) TEM image and (b) size distribution of the sample S2

The absorption spectra of the $CdSe_xS_{1-x}$ QDs for the samples are shown in Fig.2. As indicated by three arrows in Fig.2(a), the peak wavelengths of exciton absorption are 493 nm, 525 nm and 565 nm for S1, S2 and S3, respectively. The effective bandgaps of $CdSe_xS_{1-x}$ QDs were estimated to be 2.51 eV, 2.37 eV and 2.20 eV. The effective bandgaps of CSQDs samples were estimated to be 2.48 eV, 2.33 eV and 2.16 eV according to their absorption, of which the absorption spectra were not given here. Since the radius R is only about 2 nm, the strong confinement regime is considered. Based on the quantum confinement theory and empirical formula of ternary alloy semiconductor, the components x of these QDs is determined to be 0.3, 0.5 and 0.8 for S1, S2 and S3, respectively[15-17]. The composition, the blue-shifted wavelength and energy of these QDs relative to bulk counterpart are summarized in Tab.1. Their effective bandgaps relative to bulk counterparts show a sharp blue shift, which demonstrates the strong quantum confinements. In addition, the absorption peaks of these QDs show a red shift with the increase of Se composition, which indicates the composition-tuned absorption of these QDs. Relative to their bulk counterparts, the blue shifts of the effective bandgaps of these QDs get larger and larger with increase of the Cd composition and those of their $CdSe_xS_{1-x}$/ZnS CSQDs show the same trend, as shown in Tab.1. Fig.2(b) shows the comparison of S2' ($CdSe_{0.5}S_{0.5}$/ZnS) and S2 ($CdSe_{0.5}S_{0.5}$) QDs. Compared with $CdSe_{0.5}S_{0.5}$, these $CdSe_{0.5}S_{0.5}$/ZnS CSQDs exhibit a red shift of 12 nm, corresponding to the red-shifted bandgap of 36 meV, as shown in Tab.1, which indicates that the dielectric confinement effect results from the ZnS shell encapsulated on $CdSe_{0.5}S_{0.5}$ QDs. In a word, both $CdSe_xS_{1-x}$ QDs and $CdSe_xS_{1-x}$/ZnS CSQDs show the composition-tuned absorption properties.

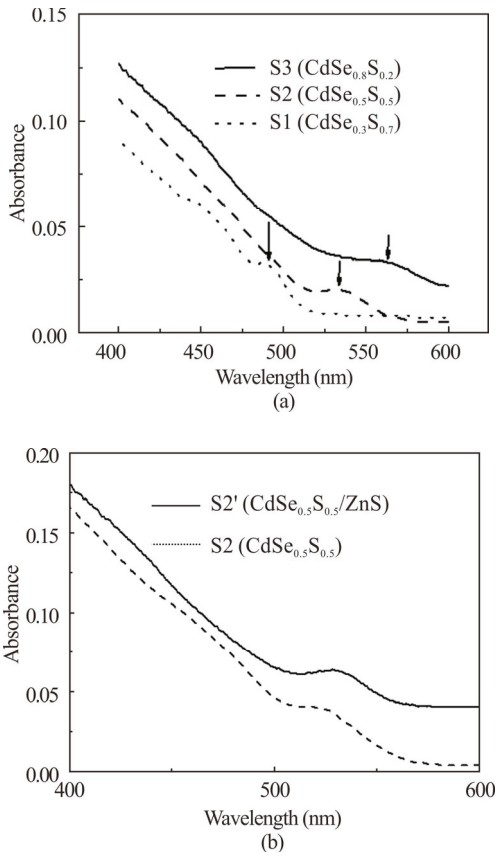

Fig.2 (a) Absorption spectra of the $CdSe_xS_{1-x}$ QDs for the samples S1, S2 and S3; (b) The comparison of absorption for S2' ($CdSe_{0.5}S_{0.5}$/ZnS) and S2 ($CdSe_{0.5}S_{0.5}$) QDs

Tab.1 Composition of $CdSe_{1-x}S_x$ QDs and their corresponding CSQDs

Sample	S1	S1'	S2	S2'	S3	S3'
Core QDs | CSQDs	$CdSe_{0.3}S_{0.7}$	$CdSe_{0.3}S_{0.7}$/ZnS	$CdSe_{0.5}S_{0.5}$	$CdSe_{0.5}S_{0.5}$/ZnS	$CdSe_{0.8}S_{0.2}$	$CdSe_{0.8}S_{0.2}$/ZnS
Blue-shifted wavelength (nm)	77	70	100	88	102	91
Blue-shifted energy (meV)	311	261	317	281	331	287

The normalized fluorescent spectra of $CdSe_{1-x}S_x$ QDs and $CdSe_{1-x}S_x$/ZnS CSQDs were shown in Fig.3(a) and Fig.3(b), respectively. There are six narrow band fluorescent spectra for the series of $CdSe_{1-x}S_x$ QDs and $CdSe_{1-x}S_x$/ZnS CSQDs, and their half width was about 36 nm, of which the narrow band emission means the high colorimetric purity. Moreover, with increase of Cd composition, the fluorescent emission of $CdSe_{1-x}S_x$ QDs and $CdSe_{1-x}S_x$/ZnS CSQDs gradually moved to the long wave direction, which implies that the fluorescent emission can be tuned by the component ratio. The excellent colorimetric purity and composition-tuned emission perhaps allow them to be used in the multi-color illumination and light emitting diode (LED) display. As for the mechanism of spectrum broadening, the particle size distribution may play an important role in the emission spectrum broadening in our opinion, and we will discuss them elsewhere in detail.

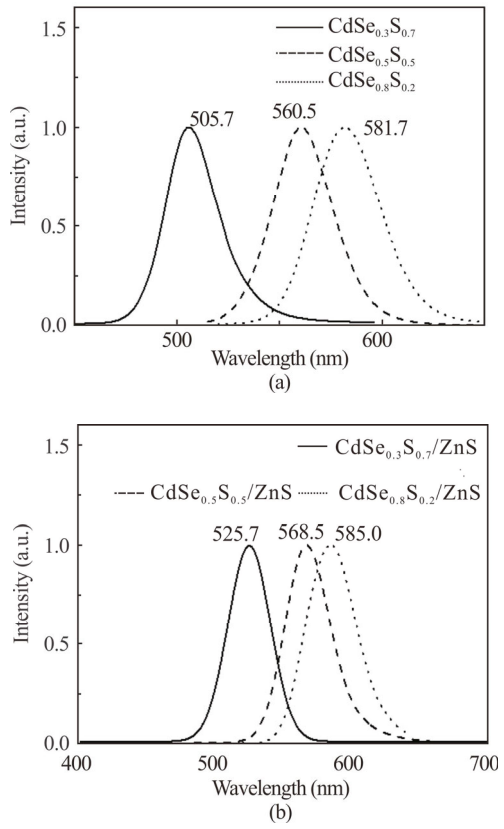

Fig.3 Normalized fluorescent spectra of (a) $CdSe_{1-x}S_x$ QDs and (b) $CdSe_{1-x}S_x$/ZnS CSQDs

In order to investigate the fluorescent chromaticity of these $CdSe_{1-x}S_x$ QDs and $CdSe_{1-x}S_x$/ZnS CSQDs, their color coordinates were obtained on the basis of their emission spectra and CIE standard[18]. As shown in Fig.4, the CIE coordinate positions of these QDs were marked with solid dots and the coordinate values were recorded in brackets. All the coordinate positions of these QDs were relatively close to the border of the chromatic diagram. And even those of some QDs almost located at the tongue curve, including $CdSe_{0.5}S_{0.5}$ QDs, $CdSe_{0.8}S_{0.2}$ QDs, $CdSe_{0.5}S_{0.5}$/ZnS CSQDs and $CdSe_{0.8}S_{0.2}$/ZnS CSQDs. These results indicate that the fluorescent emissions of these QDs were of high colorimetric purity, which is consistent with their narrow band emission. Compared the coordinates of the $CdSe_{1-x}S_x$ QDs with those of $CdSe_{1-x}S_x$/ZnS CSQDs, the obvious red shift was observed owing to ZnS shell coating. It was worth noting that the ZnS shell encapsulated on $CdSe_{0.3}S_{0.7}$ QDs not only leads to a bit red shift but also an improvement of the high colorimetric purity as shown in Fig.4(a) and Fig.4(d). As given in Fig.4, the coordinates of these QDs were tuned by the component ratios. As well known, the chromaticity of light source depends on the spectrum power distribution and the human visual function. The chromaticity simulation is significant for LED display technology, and also contributes to understanding the relationship between the chromaticity and the spectrum power distribution.

For sake of investigating the effect of shell on the optical properties, it is necessary to compare the fluorescent emission of $CdSe_{1-x}S_x$ QDs with that of $CdSe_{1-x}S_x$/ZnS CSQDs. As shown in Fig.5, the fluorescent enhancement was observed in the $CdSe_{0.8}S_{0.2}$/ZnS CSQDs in comparsion with those of the conterparts without shell layer. We also observed the fluorescent enhancement phenomena in the other two components of QDs, of which the comparison of the fluorescent spectra is similar to Fig.5 and is not given here. In the fundamental photophysical process, the emission intensity I_{PL} can be discribed by the following expression[19]

$$I_{PL}=I_0[1-(1-R)^2\exp(1-\alpha d)]\eta^*\eta_{in}, \quad (1)$$

where R is reflection coefficient, α is linear absorption

coefficient, d is the sample thickness, η_{in} is inherent fluorescence quantum yield, and η^* is the optical loss induced by light scattering and reabsorption. For exciton fluorescence, the inherent fluorescence quantum yield η_{in} can be expressed by the following formula[19]

$$\eta_{in}=\frac{\tau_s}{\tau_{ex}}=\frac{Bn}{\sigma_s \upsilon N_s}, \tag{2}$$

where $\tau_{ex}=1/Bn$ is the exciton lifetime with recombination coefficient B and exciton density n, $\tau_s=1/\sigma_s \upsilon N_s$ is non-radiative lifetime of carriers with cross section σ_s for the carriers captured by the surface traps, υ is the thermal velocity of carrier, and N_s is the surface trap concentration. As a rule, B, σ_s and υ don't depend on N_s. As shown in Eq.(2), there are two possible ways to increase η_{in}. One way is increasing the concentration (n) of excitons while fixing N_s value, and the other is decreasing N_s at constant excitation conditions. In our case, the shell coating on QDs may play a great role in the fluorescent enhancement obviously and results in the decrease of surface trap concentration N_s.

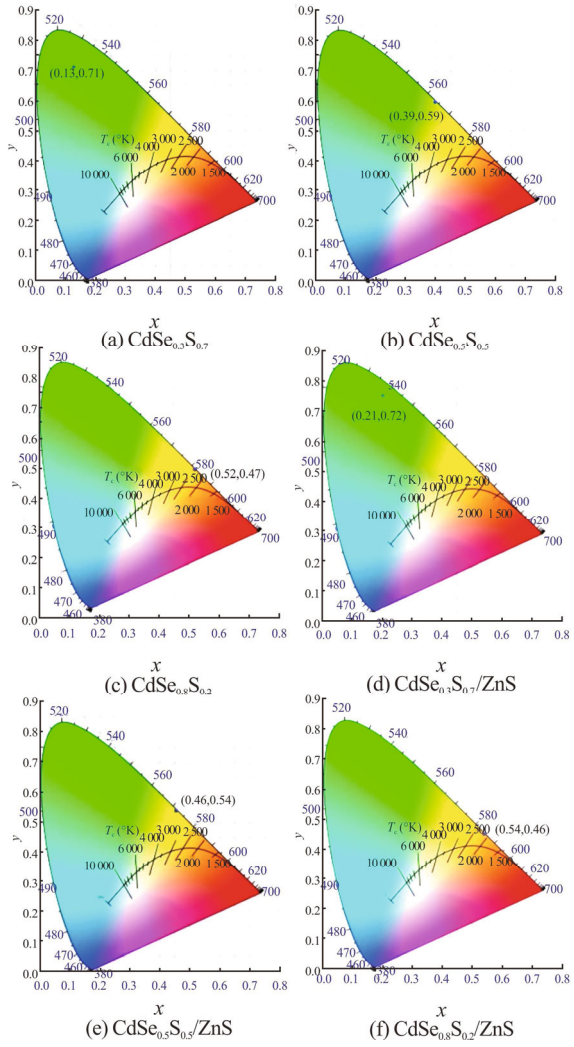

Fig.4 Chromaticity diagrams of these $CdSe_{1-x}S_x$ QDs and $CdSe_{1-x}S_x$/ZnS CSQDs

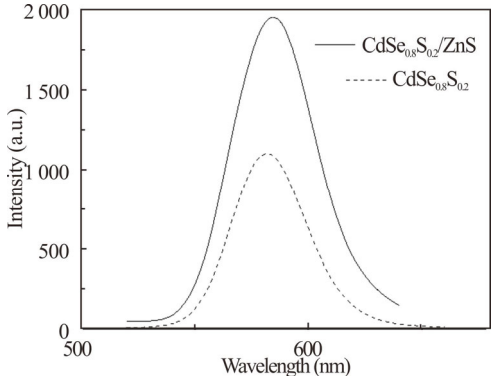

Fig.5 Comparison of the fluorescent spectra for $CdSe_{0.8}S_{0.2}$ and $CdSe_{0.8}S_{0.2}$/ZnS QDs

In summary, the optical properties of these $CdSe_{1-x}S_x$ QDs and $CdSe_{1-x}S_x$/ZnS CSQDs were investigated by the absorption and fluorescent measurement. The absorption and fluorescent emission can be tuned by the component ratio of Se and S. Based on their emission spectra and CIE standard, the color coordinates of these $CdSe_{1-x}S_x$ QDs and $CdSe_{1-x}S_x$/ZnS CSQDs were obtained by simulations. It was found that the ZnS shell encapsulated on QDs may play a great role in the emission enhancement. The composition-tuned optical properties and high colorimetric purity of these QDs perhaps lead to potential application in the photoelectric and biological fields. In addition, the chromaticity simulation also helps to understand the concept of chromaticity.

Statements and Declarations

The authors declare that there are no conflicts of interest related to this article.

References

[1] OMASULO M, YILDIZ I, RAYMO F M. pH-sensitive quantum dots[J]. Journal of physical chemistry B, 2006, 110(9): 3853-3855.

[2] HI C, BEECHER A N, LI Y, et al. Size-dependent lattice dynamics of atomically precise cadmium selenide quantum dots[J]. Physical review letters, 2019, 122: 026101.

[3] IN X, XIE K, ZHANG T, et al. Cation exchange assisted synthesis of ZnCdSe/ZnSe quantum dots with narrow emission line widths and near-unity photoluminescence quantum yields[J]. Chemical communications, 2020, 56(45): 6130-6133.

[4] AZDANI N, ANDERMATT S, YAREMA M, et al. Charge transport in semiconductors assembled from nanocrystal quantum dots[J]. Nature communications, 2020, 11(1): 2852.

[5] ELNYCHUK C, GUYOT-SIONNEST P. Multicarrier

dynamics in quantum dots[J]. Chemical reviews, 2021, 121(4)：2325-2372.

[6] AI X, ZHANG Z, JIN Y, et al. Solution-processed, high-performance light-emitting diodes based on quantum dots[J]. Nature, 2014, 515：96-99.

[7] IM J, PARK Y S, KLIMOV V I. Optical gain in colloidal quantum dots achieved with direct-current electrical pumping[J]. Nature materials, 2018, 17：42-49.

[8] RQUERFP D, TALAPIN D V, KLIMOV V I, et al. Semiconductor quantum dots：technological progress and future challenges[J]. Science, 2021, 373(6555)：1-14.

[9] EN Q, MA Y, ZHANG S, et al. One-step synthesis of water-soluble silver sulfide quantum dots and their application to bioimaging[J]. ACS omega, 2021, 6(9)：6361-6367.

[10] U Y, HAN T T, AGREN H, et al. Design of semiconductor CdSe core ZnS/CdS multishell quantum dots for multiphoton applications[J]. Applied physics letters, 2007, 90：173102.

[11] I B, KOLEY S, SLOBODKIN I, et al. ZnSe/ZnS core/shell quantum dots with superior optical properties through thermodynamic shell growth[J]. Nano letters, 2020, 20(4)：2387-2395.

[12] ANN T, SKINNER W M. Quantum dots for electro-optic devices[J]. ACS nano, 2011, 5(7)：5291-5295.

[13] IM S H, MAN M T, LEE J W, et al. Influence of size and shape anisotropy on optical properties of CdSe quantum dots[J]. Nanomaterials, 2020, 10：1589.

[14] IJAZ P, IMRAN M, SOARES M M, et al. Composition-, size-, and surface functionalization-dependent optical properties of lead bromide perovskite nanocrystals[J]. Journal of physical chemistry letters, 2020, 11(6)：2079-2085.

[15] HAO S, WU F, ZHANG S, et al. Components-dependent optical nonlinearity in a series of $CdSe_xS_{1-x}$ and $CdSe_xS_{1-x}$/ZnS QDs[J] . Optics and laser technology, 2016, 82：104-107.

[16] APRA S, SARMA D D. Evolution of the electronic structure with size in II-VI semiconductor nanocrystals[J]. Physical review B, 2004, 69：125304.

[17] ERNA G, PAGLIARA S, CAPOZZI V, et al. Optical characterization of CdS_xSe_{1-x} films grown on quartz substrate by pulsed laser ablation technique[J]. Thin solid films, 1999, 349：220-224.

[18] ING Q C, JIAO S L. Colourometry[M]. Beijing：Science Press, 1979. (in Chinese)

[19] UNETSV P, KULISHN R, STRELCHUKV V, et al. CdS Se quantum dots：effect of the hydrogen RF plasma treatment on exciton luminescence[J]. Physica E, 2004, 22：804-807.